# MACHINE LEARNING FOR PREDICTING THE DYNAMICS OF INFECTIOUS DISEASES DURING TRAVEL THROUGH PHYSICS INFORMED NEURAL NETWORKS

Alonso G. Ogueda-Oliva,<sup>1</sup> Erika Johanna Martínez-Salinas,<sup>2</sup> Viswanathan Arunachalam,<sup>2</sup> & Padmanabhan Seshaiyer<sup>1,\*</sup>

Original Manuscript Submitted: 12/15/2022; Final Draft Received: 7/6/2023

In the past few years, approaches such as physics informed neural networks (PINNs) have been applied to a variety of applications that can be modeled by linear and nonlinear ordinary and partial differential equations. Specifically, this work builds on the application of PINNs to a SIRD (susceptible, infectious, recovered, and dead) compartmental model and enhances it to build new mathematical models that incorporate transportation between populations and their impact on the dynamics of infectious diseases. Our work employs neural networks capable of learning how diseases spread, forecasting their progression, and finding their unique parameters. We show how these approaches are capable of predicting the behavior of a disease described by governing differential equations that include parameters and variables associated with the movement of the population between neighboring cities. We show that our model validates real data and also how such PINNs based methods predict optimal parameters for given datasets.

**KEY WORDS:** compartmental models, epidemiology, neural networks, transport, deep learning

## 1. INTRODUCTION

The outbreak of COVID-19 and its variants has since spread across the globe to over 200 countries and territories. As of July 2021, over 185 million cases and 4 million deaths worldwide were due to COVID-19, as the World Health Organization reported in Coronavirus (2021). The pandemic has changed human relationships and social interactions due to measures such as mandatory isolation, restricted purchase of essential items, closure of significant public events, and closure of educational centers. People have had to experience changes in the way people

<sup>&</sup>lt;sup>1</sup>Department of Mathematical Sciences, George Mason University, Fairfax, Virginia 22030, USA

<sup>&</sup>lt;sup>2</sup>Departamento de Estadística, Facultad de Ciencias, Universidad Nacional de Colombia, Bogotá 111321, Colombia

<sup>\*</sup>Address all correspondence to: Padmanabhan Seshaiyer, Department of Mathematical Sciences, George Mason University, Fairfax, Virginia 22030, USA, E-mail: pseshaiy@gmu.edu

communicate, in how they learn, or in the way inhabitants of different regions travel and communicate, even in the same territory. With travel that has resumed again, there is now potential for more interaction in populations moving within and between cities. For this reason, understanding the dynamics of disease transmission continues to be a problem of global interest.

Different methodologies and approaches have been used to model and predict the spread of infectious diseases, for example, deterministic epidemiological models which use systems of ordinary differential equations such as SIR (susceptible, infected, and recovered), SIS (susceptible and infected), and SEIR (susceptible, exposed, infected, and recovered). The first epidemiological mathematical model was developed to study influenza using an SIR model (Kermack and McKendrick, 1927). In this model, three types of individuals are distinguished: the susceptible, the infected, and the removable. Susceptible individuals are those who are likely to catch a disease by having infectious contact with infected individuals who may or may not present symptoms of the disease. Removable individuals are those who are no longer infected. Following the influenza pandemic, several countries and leading organizations increased funding and attention to finding cures for infectious diseases in the form of vaccines and medicines. Along with these policy implementations, newer modified SIR models for mathematical epidemiology continued to evolve, particularly for those diseases that are categorized as reemerging infections that spread through sexual transmission, such as HIV (Castillo-Chavez, 2013), through vectors such as mosquitoes, e.g., malaria or dengue (Chowell et al., 2007), through both sexual and vector transmissions, such as Zika (Padmanabhan et al., 2017), and those that can be spread by viruses, including SARS (Dye and Gay, 2003).

While there have been significant advances in mathematical modeling of infectious diseases, there is a great need to develop efficient and fast computational techniques for estimating parameters in these associated differential equation systems (Raissi et al., 2019b). One of the promising approaches is the physics informed neural networks (PINNs) where neural networks are trained to solve supervised learning tasks while respecting any given law of physics described by general nonlinear partial differential equations (Raissi et al., 2019a). Specifically, the mechanism solves two problems: the solution based on data and the discovery of partial differential equations based on data. Other methodologies have emerged, such as those studied in Yazdani et al. (2020), where the system of ordinary differential equations (ODEs) is incorporated into neural networks, effectively adding constraints to the optimization algorithm, which makes the method robust for scarce and noisy measurements. Many of these works focus on understanding the operation of differential equations that learn from data. Recently, a unified approach called DINNs (disease informed neural networks) was introduced where an approach can be employed to effectively predict the spread of infectious diseases; is presented in Shaier et al. (2022).

In this work, we focus on expanding the study of DINNs by analyzing different scenarios using modified SIRD compartmental models and including the disease transmission rate incorporating individuals' transport between the two crowded neighboring cities. Specifically, the motivation comes from Colombia and its two main cities, the largest city, Bogotá, and Medellín, the second-most populated city with industrial, business, and commercial activities. People travel between these cities for business, family, and vacation. The estimated flight time is approximately 55 minutes.

The paper is structured as follows. In Section 2, we review the necessary background information. Section 3 shows the application of the proposed method to some benchmark applications involving both synthetic data and real data from Colombia. Finally, we conclude with discussion and conclusions in Section 4.

### 2. MODELS AND BACKGROUND

Over the past several decades, compartmental models have been employed with mathematical modeling to study the spread of infectious diseases (Brauer et al., 2012). As mentioned before, one of the original mathematical conceptualizations of how disease spreads is an SIR model that was introduced to describe the interaction between susceptible (S), infectious (I), and recovered (R) human sub-populations (Kermack and McKendrick, 1927). A modified version of this model is the SIRD model, where a dead (D) compartment is also introduced, and its dynamics are also studied along with the other three compartments. This model was used to describe one of the earlier models for understanding COVID-19 spread in Italy (Calafiore et al., 2020). This is illustrated by the flow diagram in Fig. 1, where  $\beta$ ,  $\omega$ , and  $\gamma$  are the rates of infection, recovery, and mortality, respectively. This can be modeled as a system of differential equations:

$$\dot{S} = -\beta \frac{S}{N} I,\tag{1a}$$

$$\dot{I} = \beta \frac{S}{N} I - \omega I - \gamma I, \tag{1b}$$

$$\dot{R} = \omega I,$$
 (1c)

$$\dot{D} = \gamma I. \tag{1d}$$

Here we have assumed that N=S+I+R+D is the total human population. It is assumed that susceptible individuals S move to the infected class I after acquiring the COVID-19 disease through interaction with an infected individual. This transmission is being modeled via the addition of terms directly proportional to the respective infected human classes I involved in the transmission and an infection rate proportional to the infected individuals. The rate of transmission from the infected to susceptible humans is given by the usual product  $\beta$ . Members of the infected class I can either recover with a rate proportional to  $\omega$ , moving to the recovered class, or move to the death compartment with a rate of  $\gamma$ . Next we expand this model to include the impact of transportation which is one of the motivations of this work.

# 2.1 Adding Transportation

The flow diagram in Fig. 1 considers only one population. Motivated by Hernández et al. (2016), we expand the SIRD model to include transportation to study the spread of COVID-19. Specifically, we consider a transportation matrix for two population regions given by

$$\begin{pmatrix} 0 & \tau_{1,2} \\ \tau_{2,1} & 0 \end{pmatrix}$$
,

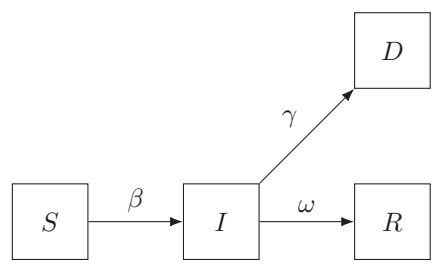


FIG. 1: Classical SIRD flow diagram

where each  $\tau_{i,j}$  represents the flux of transportation from region i to region j, where i, j = 1, 2. Then the associated flow diagram for a new compartmental model this scenario can be modeled as Fig. 2. Its corresponding system of differential equations follows:

$$\dot{S}_1 = -\beta_1 \frac{S_1}{N_1} I_1 - \tau_{1,2} S_1 + \tau_{2,1} S_2, \tag{2a}$$

$$\dot{I}_{1}=\beta_{1}\frac{S_{1}}{N_{1}}I_{1}-\omega_{1}I_{1}-\gamma_{1}I_{1}-\tau_{1,2}I_{1}+\tau_{2,1}I_{2}, \tag{2b} \label{eq:2b}$$

$$\dot{R}_1 = \omega_1 I_1 - \tau_{1,2} R_1 + \tau_{2,1}, R_2, \tag{2c}$$

$$\dot{D_1} = \gamma_1 I_1,\tag{2d}$$

$$\dot{S}_2 = -\beta_2 \frac{S_2}{N_2} I_2 - \tau_{2,1} S_2 + \tau_{1,2} S_1, \tag{2e}$$

$$\dot{I}_2 = \beta_2 \frac{S_2}{N_2} I_2 - \omega_2 I_2 - \gamma_2 I_2 - \tau_{2,1} I_2 + \tau_{1,2} I_1, \tag{2f}$$

$$\dot{R}_2 = \omega_2 I_2 - \tau_{2,1} R_2 + \tau_{1,2} R_1, \tag{2g}$$

$$\dot{D}_2 = \gamma_2 I_2. \tag{2h}$$

## 2.2 Transportation with Short-Term Cross Transmission

System (2) does not consider the interaction between people from different regions. Since we are modeling short-term travel, for example, people who commute to work, we introduce two new parameters. First of all,  $\delta_{i,j}$  is the rate of infection among people who travel from region i to region j but susceptible individuals from i interact with infected individuals from i, for example, when commuting in the morning in a bus or train. Secondly,  $\zeta_{i,j}$  is the rate of infection between people who travel from region i to region j but individuals from i interact with infected

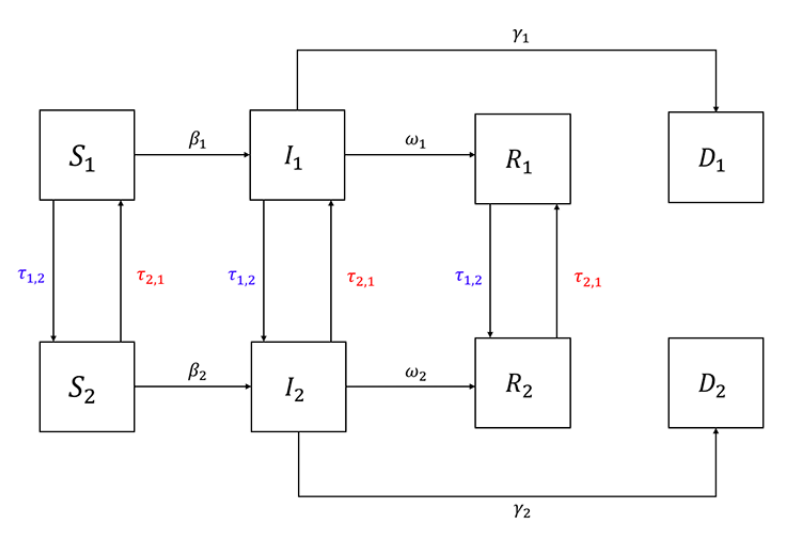


FIG. 2: SIRD model with transportation flow diagram

individuals of j, for example, interaction in an office, school, etc. The associated flow diagram for this scenario can be modeled as Fig. 3. The system of governing differential equations for Fig. 3 is as follows:

$$\dot{S}_{1} = -\beta_{1} \frac{S_{1}}{N_{1}} I_{1} - \tau_{1,2} S_{1} + \tau_{2,1} S_{2} - \zeta_{1,2} \frac{S_{1}}{N_{1}} I_{2} - \delta_{1,2} \frac{S_{1}}{N_{1}} I_{1}, \tag{3a}$$

$$\dot{I}_{1} = \beta_{1} \frac{S_{1}}{N_{1}} I_{1} - \omega_{1} I_{1} - \gamma_{1} I_{1} - \tau_{1,2} I_{1} + \tau_{2,1} I_{2} + \zeta_{1,2} \frac{S_{1}}{N_{1}} I_{2} + \delta_{1,2} \frac{S_{1}}{N_{1}} I_{1},$$
 (3b)

$$\dot{R}_1 = \omega_1 I_1 - \tau_{1,2} R_1 + \tau_{2,1} R_2, \tag{3c}$$

$$\dot{D}_1 = \gamma_1 I_1,\tag{3d}$$

$$\dot{S}_{2} = -\beta_{2} \frac{S_{2}}{N_{2}} I_{2} - \tau_{2,1} S_{2} + \tau_{1,2} S_{1} - \zeta_{2,1} \frac{S_{2}}{N_{2}} I_{1} - \delta_{2,1} \frac{S_{2}}{N_{2}} I_{2}, \tag{3e}$$

$$\dot{I}_{2} = \beta_{2} \frac{S_{2}}{N_{2}} I_{2} - \omega_{2} I_{2} - \gamma_{2} I_{2} - \tau_{2,1} I_{2} + \tau_{1,2} I_{1} + \zeta_{2,1} \frac{S_{2}}{N_{2}} I_{1} + \delta_{2,1} \frac{S_{2}}{N_{2}} I_{2},$$
 (3f)

$$\dot{R}_2 = \omega_2 I_2 - \tau_{2,1} R_2 + \tau_{1,2} R_1, \tag{3g}$$

$$\dot{D}_2 = \gamma_2 I_2. \tag{3h}$$

Table 1 defines each parameter in the model.

## 2.3 Derivation of the Basic Reproduction Number

When studying the dynamics of a certain disease, it is important to estimate the speed with which it can spread in a population, a measure known as the basic reproductive number, notated as  $\mathcal{R}_0$ , which is defined as the average number of secondary infections produced by a typical case of an infection in a population where everyone is susceptible (Diekmann et al., 1990). This

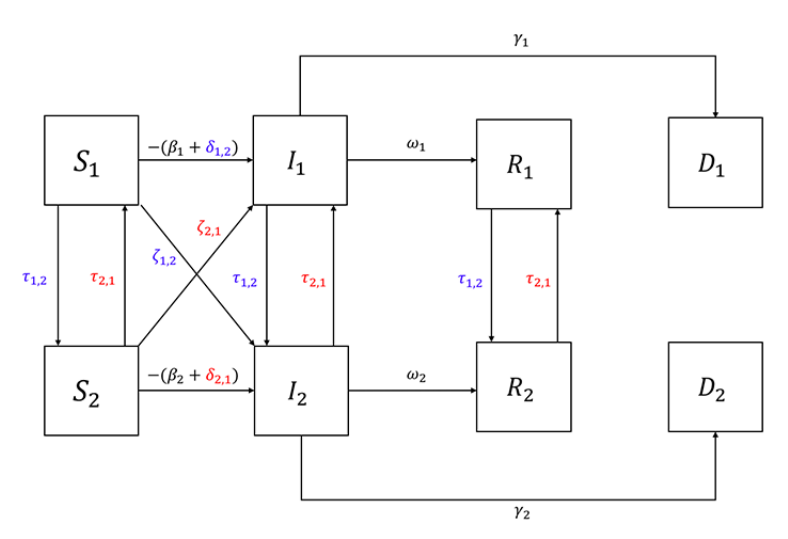


FIG. 3: SIRD model with transportation and cross transmission flow diagram

**TABLE 1:** Parameter definition of model (3)

Parameter	Definition
$\beta_i$	Transmission rate
	Rate of infection between people who travel from region
$\delta_{i,j}$	i to region $j$ but susceptible individuals from $i$
	interact with infected individuals from $i$
	Rate of infection between people who travel from region
$\zeta_{i,j}$	i to region $j$ but individuals from $i$ interact with
	infected individuals of j
$\omega_i$	Rate at which individuals become recovered
$\xi_{,i}$	Rate at which symptomatic individuals become quarantined
$\gamma_i$	Rate at which infected individuals become dead
$ au_{i,j}$	Transport rate between two regions

number is a measure of the potential for disease spread within a population (Van den Driessche and Watmough, 2008).

In this section, we will derive a basic reproduction number  $\mathcal{R}_0$  to measure the transmission potential of COVID-19 as proposed by the system of Eq. (2).

Model (2) includes sub-populations with different infectious states; therefore, we have employed a general approach called the *next generation matrix* (Brauer et al., 2012) to find the basic reproduction number  $\mathcal{R}_0$  which is given by the following equations.

Given the infectious states  $I_1$ ,  $I_2$  in system (2), we can create a vector  $\mathcal{F}$  that represents the new infections flowing only into the exposed compartments given by

$$\mathcal{F} = (\beta_1 I_1 + \tau_{2,1} I_2, \ \beta_2 I_2 + \tau_{1,2} I_1)^{\top}. \tag{4}$$

Along with  $\mathcal{F}$ , we will also consider  $\mathcal{V}$  which denotes the outflow from the infectious compartments in the system of equations (2) which is given by

$$\mathcal{V} = (\omega_1 I_1 + \gamma_1 I_1 + \tau_{1,2} I_1, \ \omega_2 I_2 + \gamma_2 I_2 + \tau_{2,1} I_2)^{\top}. \tag{5}$$

Next, we compute the Jacobian F from  $\mathcal{F}$  given by

$$F = \left(\begin{array}{cc} \beta_1 & \tau_{2,1} \\ \tau_{1,2} & \beta_2 \end{array}\right),$$

and the Jacobian V from V given by

$$V = \begin{pmatrix} \omega_1 + \gamma_1 + \tau_{1,2} & 0 \\ 0 & \omega_2 + \gamma_2 + \tau_{2,1} \end{pmatrix}.$$

We can then compute the inverse of the matrix V to be

$$V^{-1} = \begin{pmatrix} \frac{1}{\omega_1 + \gamma_1 + \tau_{1,2}} & 0\\ 0 & \frac{1}{\omega_2 + \gamma_2 + \tau_{2,1}} \end{pmatrix}.$$

Using matrices F and V one can then compute the next generation matrix  $FV^{-1}$  given by

$$FV^{-1} = \begin{pmatrix} \frac{\beta_1}{\omega_1 + \gamma_1 + \tau_{1,2}} & \frac{\tau_{2,1}}{\omega_2 + \gamma_2 + \tau_{2,1}} \\ \\ \frac{\tau_{1,2}}{\omega_1 + \gamma_1 + \tau_{1,2}} & \frac{\beta_2}{\omega_2 + \gamma_2 + \tau_{2,1}} \end{pmatrix}.$$

Note that the (i,j) entry of the next generation matrix  $FV^{-1}$  is the expected number of secondary infections in compartment i produced by individuals initially in compartment j assuming that the environment seen by the individual remains homogeneous for the duration of their infection. Also, matrix  $FV^{-1}$  is non-negative and therefore has a non-negative eigenvalue. The basic reproduction number can then be computed as  $\mathcal{R}_0 = \rho(FV^{-1})$  which is the spectral radius of the matrix. This non-negative eigenvalue is associated with a non-negative eigenvector which represents the distribution of infected individuals that produce the greatest number  $\mathcal{R}_0$  of secondary infections per generation.

The basic reproduction number  $\mathcal{R}_0$  corresponds to the dominant eigenvalue  $\lambda$  that satisfies the following equation:

$$\lambda^2 - \lambda \left( \frac{\beta_1}{\omega_1 + \gamma_1 + \tau_{1,2}} + \frac{\beta_2}{\omega_2 + \gamma_2 + \tau_{2,1}} \right) + \frac{\beta_1 \beta_2 - \tau_{1,2} \tau_{2,1}}{(\omega_1 + \gamma_1 + \tau_{1,2})(\omega_2 + \gamma_2 + \tau_{2,1})} = 0.$$

Remark 1. Note that when  $\gamma_1 = \gamma_2 = 0$  and  $\tau_{1,2} = \tau_{2,1} = 0$ , then the basic reproduction number  $\mathcal{R}_0$  corresponds to the dominant eigenvalue  $\lambda$  that satisfies the following equation:

$$\lambda^2 - \lambda \left( \frac{\beta_1}{\omega_1} + \frac{\beta_2}{\omega_2} \right) + \frac{\beta_1 \beta_2}{\omega_1 \omega_2} = 0.$$

Solving for the roots of the quadratic equations, we have

$$\mathcal{R}_0 = \max \left\{ \frac{\beta_1}{\omega_1}, \frac{\beta_2}{\omega_2} \right\},\,$$

which corresponds to the classic result of the ratio of the transmission rate to the recovery rate of each population.

Figure 4 shows the behavior of  $R_0$  for different scenarios when we change the transmission and recovery rate corresponding to the second region. Each of its nine sub-figures is a contour plot where the axes are continuous values of  $\tau_{1,2}$  and  $\tau_{2,1}$ . We can see how by modifying these values we can observe a nonlinear relationship between  $R_0$  and the transport rates. However, it is clear than when the transmission rate is larger, then the maximum value of  $R_0$  also increases. Note that in the first row,  $R_0$  is basically between 0 and 2; however, the third row shows values between around 1.5 and 3.

#### 2.4 Parameter Estimation

One of the challenges in using compartmental models with an associated differential equation system to describe the dynamics is the *estimation of parameters* for the given data. Usually, parameters may be estimated from observing patterns in the data, but transmission rates often have to be computed using heuristic algorithms that are computationally or statistically motivated. In

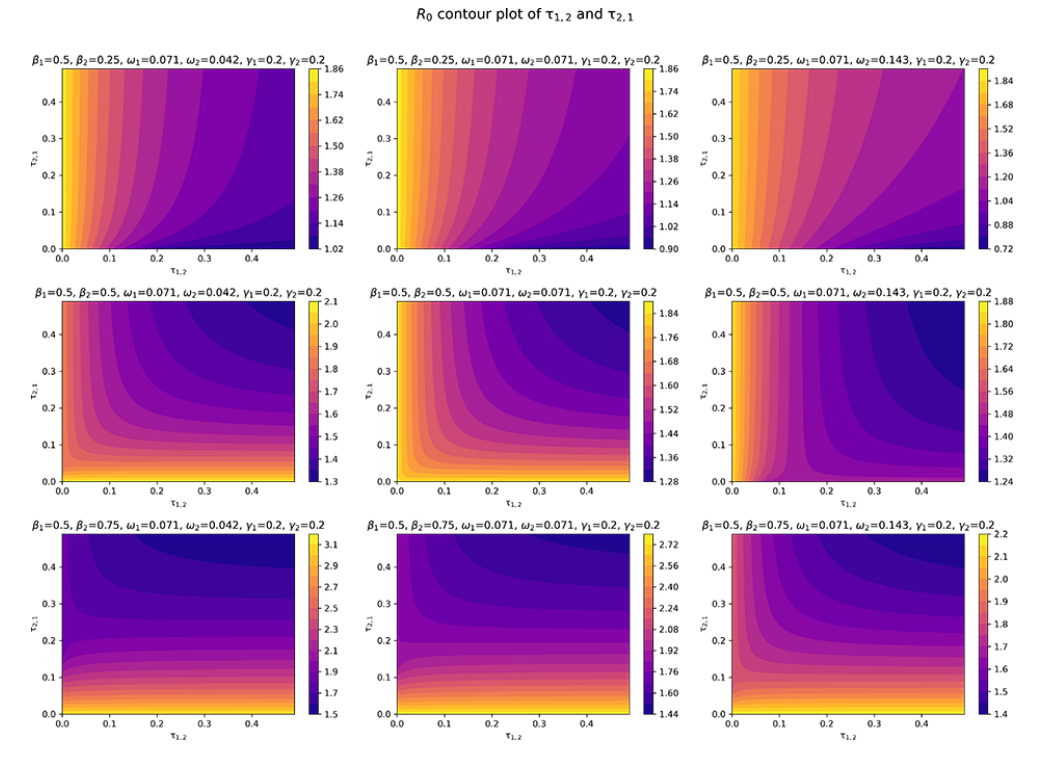


**FIG. 4:**  $R_0$  value (colorized) for different combinations of  $\tau_{1,2}$  (horizontal axis) and  $\tau_{2,1}$  (vertical axis)

recent years, there have been new approaches with *machine learning* to discover parameters in the governing equations (Raissi et al., 2019b). One of the approaches includes artificial neural networks that are motivated by the human neural system where each neuron is represented with a node, signals are inputs, and the synapse is the function evaluation. Each neuron is connected to different neurons to increase accuracy through multiple layers.

Artificial neural networks have been used in regression and classification tasks in the last few years. By adding the physics behind the given problem, i.e., the system of equations, Raissi et al. (2019a) proposed a new approach called physics-informed neural networks. These neural networks encode model equations, like partial differential equations (PDEs), as a component of the neural network itself (Cuomo et al., 2022).

This approach aims to solve two main classes of problems: *data-driven solution* and *data-driven discovery* of partial differential equations. It is a fast and mesh-free method. However, it is still in early development. Shaier et al. (2022) proposed to leverage the hidden physics of infectious diseases and infer the latent quantities of interest by approximating them using PINNs. This approach is called diseases informed neural networks (DINNs), and the architecture is similar, as we can see in Fig. 5 for a simple SIRD model.

Consider for example, the SIRD model and that we want to approximate the function  $t \longrightarrow (S, I, R, D)$ . Then the residuals of the ordinary differential equations system can be written as

$$\mathcal{L}_S = \dot{S} + \beta \frac{S}{N} I, \tag{6a}$$

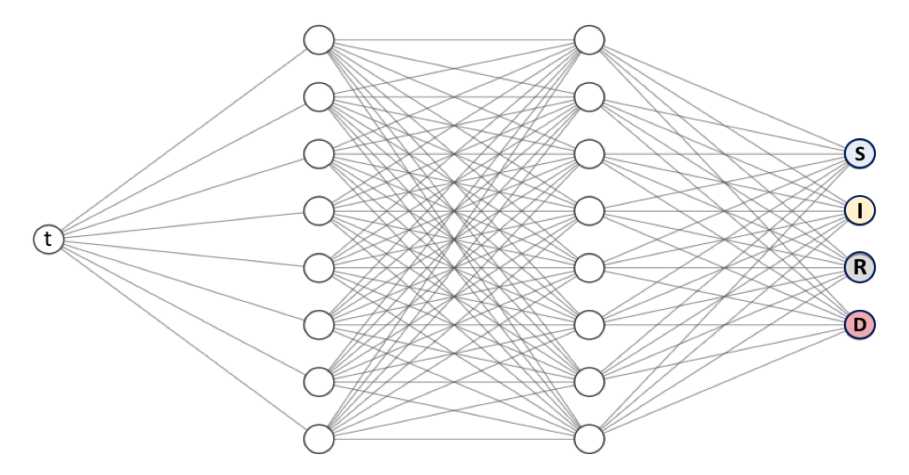


**FIG. 5:** DINNs architecture for a SIRD model. Training data are only temporal and output is *n*th dimensional depending on the number of equations/compartments.

$$\mathcal{L}_{I} = \dot{I} - \beta \frac{S}{N} I + \omega I + \gamma I, \tag{6b}$$

$$\mathcal{L}_R = \dot{R} - \omega I,\tag{6c}$$

$$\mathcal{L}_D = \dot{D} - \gamma I. \tag{6d}$$

Similarly, model (3) corresponding to transportation for short-term cross transmission has the following residuals:

$$\mathcal{L}_{S_1} = \dot{S}_1 - \left( -\beta_1 \frac{S_1}{N_1} I_1 - \tau_{1,2} S_1 + \tau_{2,1} S_2 - \zeta_{1,2} \frac{S_1}{N_1} I_2 - \delta_{1,2} \frac{S_1}{N_1} I_1 \right), \tag{7a}$$

$$\mathcal{L}_{I_1} = \dot{I}_1 - \left(\beta_1 \frac{S_1}{N_1} I_1 - \omega_1 I_1 - \gamma_1 I_1 - \tau_{1,2} I_1 + \tau_{2,1} I_2 + \zeta_{1,2} \frac{S_1}{N_1} I_2 + \delta_{1,2} \frac{S_1}{N_1} I_1\right), \quad (7b)$$

$$\mathcal{L}_{R_1} = \dot{R}_1 - (\omega_1 I_1 - \tau_{1,2} R_1 + \tau_{2,1} R_2), \tag{7c}$$

$$\mathcal{L}_{D_1} = \dot{D}_1 - \gamma_1 I_1,\tag{7d}$$

$$\mathcal{L}_{S_2} = \dot{S_2} - \left( -\beta_2 \frac{S_2}{N_2} I_2 - \tau_{2,1} S_2 + \tau_{1,2} S_1 - \zeta_{2,1} \frac{S_2}{N_2} I_1 - \delta_{2,1} \frac{S_2}{N_2} I_2 \right), \tag{7e}$$

$$\mathcal{L}_{I_2} = \dot{I_2} - \left(\beta_2 \frac{S_2}{N_2} I_2 - \omega_2 I_2 - \gamma_2 I_2 - \tau_{2,1} I_2 + \tau_{1,2} I_1 + \zeta_{2,1} \frac{S_2}{N_2} I_1 + \delta_{2,1} \frac{S_2}{N_2} I_2\right), \quad (7f)$$

$$\mathcal{L}_{R_2} = \dot{R}_2 - (\omega_2 I_2 - \tau_{2,1} R_2 + \tau_{1,2} R_1), \tag{7g}$$

$$\mathcal{L}_{D_2} = \dot{D}_2 - \gamma_2 I_2. \tag{7h}$$

One of the novelties in our work is to train a neural network with temporal data and estimate the best values of the model parameters without much prior information. Let the unknown solution be a vector of eight components such that

$$u(t;\lambda) = (S_1(t;\lambda), I_1(t;\lambda), R_1(t;\lambda), D_1(t;\lambda), S_2(t;\lambda), I_2(t;\lambda), R_2(t;\lambda), D_2(t;\lambda))^{\top},$$

where  $\lambda$  are the parameters related to disease dynamics, and a known initial condition u(0).

Using the PINNs methodology we need training data, a discretization of time, and the solution  $\{t^j\}$ ,  $\{u^j\}$  where  $j=0,1,\ldots,N_{\rm data}$  such that  $t^0=0$  is the initial time. The goal is to train a neural network with the vector of parameters  $\widehat{\lambda}$  and  $\theta$  (a vector of weights and biases for each neuron) in order to obtain an approximation  $\widehat{u}^j(\widehat{\lambda},\theta)$  using the following loss function for the optimization step of our model,

$$\mathcal{L}(\widehat{\lambda},\theta) = \omega_{ode} \mathcal{L}_{ode}(\widehat{\lambda},\theta) + \omega_{ic} \mathcal{L}_{ic}(\widehat{\lambda},\theta) + \omega_{data} \mathcal{L}_{data}(\widehat{\lambda},\theta),$$

where  $\omega_{ode}$ ,  $\omega_{ic}$ , and  $\omega_{data}$  are the loss weights of the loss functions of the system of differential equations, initial conditions, and training data, respectively. The loss function is decomposed in three other parts, where

$$\mathcal{L}_{ode}(\widehat{\lambda}, \theta) = \mathcal{L}_{S_1}(\widehat{\lambda}, \theta) + \mathcal{L}_{I_1}(\widehat{\lambda}, \theta) + \mathcal{L}_{R_1}(\widehat{\lambda}, \theta) + \mathcal{L}_{D_1}(\widehat{\lambda}, \theta) + \mathcal{L}_{S_2}(\widehat{\lambda}, \theta) + \mathcal{L}_{I_2}(\widehat{\lambda}, \theta) + \mathcal{L}_{R_2}(\widehat{\lambda}, \theta) + \mathcal{L}_{D_2}(\widehat{\lambda}, \theta),$$

is the loss function for the approximated solution, and

$$\mathcal{L}_{\text{data}}(\widehat{\lambda}, \theta) = \sum_{i=1}^{8} \frac{1}{N_{\text{data}}} \sum_{j=1}^{N_{\text{data}}} \left( u_i^j - \widehat{u}_i^j(\widehat{\lambda}, \theta) \right)^2 \quad \text{and} \quad \mathcal{L}_{\text{ic}}(\widehat{\lambda}, \theta) = \sum_{i=1}^{8} \left( u_i^0 - \widehat{u}_i^0(\widehat{\lambda}, \theta) \right)^2,$$

where i = 1, ..., 8 is a counter for each component of the solution; for example,  $(u_1, u_2, u_3, u_4)$  correspond to  $(S_1, I_1, R_1, D_1)$  and  $(u_5, u_6, u_7, u_8)$  correspond to  $(S_2, I_2, R_2, D_2)$ . Algorithm 1 shows how to predict  $u(t; \lambda)$  and the parameters  $\lambda$ .

## Algorithm 1: DINNs algorithm considering transportation between two regions

**Input**: Training Data  $\{t^j\}$ ,  $\{u^j\}$  where  $j = 0, 1, \dots, N_{\text{data}}$ 

**Output:**  $\widehat{u}$  and  $\widehat{\lambda}$ 

- 1 Initialize  $\lambda_0$  and  $\theta_0$ .
- 2 Define time interval where the solution will be found.
- 3 Define loss function  $\mathcal{L}(\hat{\lambda}, \theta)$ , related to residual errors, initial conditions, and training data.
- 4 Create a fully connected neural network with one neuron in the input layer and eight neurons in the output layer (one per compartment), and such that it normalizes the input data.
- 5 Choose optimization hyperparameters (e.g., Adam optimizer, learning rate, and loss weights).
- 6 for  $iter = 1, ..., max\_iter$  do
- 7 Compute total loss  $\mathcal{L}(\hat{\lambda}_{\mathtt{iter}-1}, \theta_{\mathtt{iter}-1})$ ; in particular it is necessary to use autodifferentiation for ODE residuals.
- 8 Train neural network with optimizer algorithm and update  $\theta_{iter-1}$  to  $\theta_{iter}$ .
- 9 Get approximation  $\widehat{u}_{iter}$  and  $\widehat{\lambda}_{iter}$ .

end

10 Return  $\widehat{u}_{\text{max\_iter}}$  and  $\widehat{\lambda}_{\text{max\_iter}}$ .

## 3. NUMERICAL EXPERIMENTS

For numerical computations we used Python as a programming language, but in particular the package <code>DeepXDE</code> (https://github.com/lululxvi/deepxde) as our main tool for PINNs, since it has the flexibility for working with a system of ODEs.

## 3.1 Synthetic Data

For validation, we generated synthetic data with specific parameters, which allows us to measure the parameter error of the model. For this purpose, since the parameters are known we solved the system of differential equations using the Python package <code>scipy</code>, specifically the function <code>scipy.integrate.odeint</code>, which uses <code>LSODA</code> from the FORTRAN library <code>odepack</code>. From here, we have the real values of each parameter and each compartment in every time t from 0 to 366 (in order to simulate an entire year).

We executed the model several times with different hyperparameters related to the neural network architecture in order to obtain the best error. Specifically, we employed 30,000 iterations with three and five layers. We considered the number of neurons per layer to be 32, 64, and 128. For our simulations we employed the rectified linear units (ReLU) as the activation function. The main advantage of using the ReLU function over other activation functions is that it does not activate all the neurons at the same time. This means that the neurons will only be deactivated if the output of the linear transformation is less than 0. For the weights in the respective loss functions, combinations of 1 and 10 were employed between the observed data, initial conditions, and ODEs loss.

In the same way as Yazdani et al. (2020), the range for parameter searching is set as (0.2p, 1.8p), where p is a nominal value of each parameter. Figures 6 and 7 show us the training data (dots) and the full prediction (line) in each sub-population without and with short-term cross transmission, respectively. As we can see in Tables 2 and 3 we obtained in general really good approximations of the parameters. In particular, we are interested in parameters which modeled nonlinear behaviors such as  $\beta_i$ ,  $\delta_{i,j}$ , or  $\zeta_{i,j}$  where we got relatively small errors. However, in the short-term cross transmission experiment we can see that  $\tau_{i,j}$  parameters did not do well.

#### 3.1.1 Noise

Next, to study the robustness of the model, we considered adding noise of 5% and 10%, respectively to the synthetic data and simulated DINNs framework. Figures 8 and 9 seem to indicate that our method is reliable and robust. Also, we notice that as the amount of noise decreases, the performance of the method improves.

#### 3.1.2 Missing Observations

Our next experiment was to simulate the behavior in the present data with missing values. For instance, we considered a situation where we did not include the infected sub-population in the training process. Figure 10 shows that even without that data the method was able to get a good approximation.

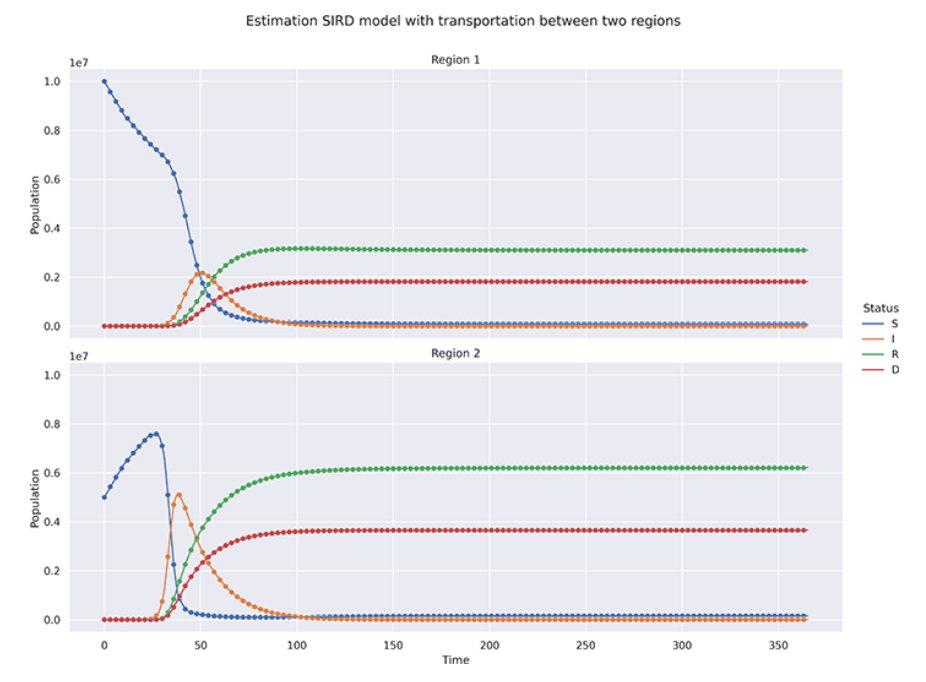
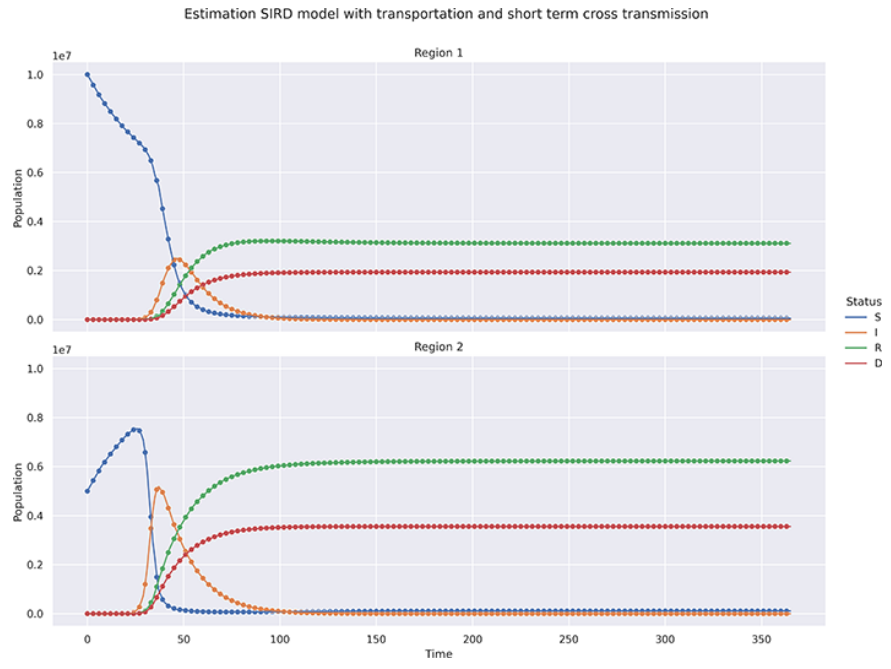


FIG. 6: SIRD with transportation model, training (dots), and prediction (line) using synthetic data



**FIG. 7:** SIRD with transportation and short-term cross transmission model, training (dots), and prediction (line) using synthetic data

**TABLE 2:** Parameter predictions and relative errors for SIRD with transportation

Parameter	Real	Predicted	Relative Error
$\beta_1$	0.45	0.450849559	0.001887908
$\omega_1$	0.05	0.050518012	0.010360249
$\gamma_1$	0.0294	0.029936808	0.018258763
$\beta_2$	0.4	0.479594968	0.198987419
$\omega_2$	0.05	0.053104374	0.062087473
$\gamma_2$	0.0294	0.031391702	0.067744976
$ au_{1,2}$	0.02	0.019206325	0.03968376
$ au_{2,1}$	0.01	0.009627349	0.037265099

**TABLE 3:** Parameter predictions and relative errors for SIRD with transportation and short-term cross transmission

Parameter	Real	Predicted	Relative Error
$\beta_1$	0.45	0.480948498	0.06877444
$\omega_1$	0.05	0.048348768	0.033024639
$\gamma_1$	0.0294	0.028237397	0.039544315
$\beta_2$	0.4	0.409425762	0.023564406
$\omega_2$	0.05	0.050155453	0.003109051
$\gamma_2$	0.0294	0.029991729	0.020126824
$ au_{1,2}$	0.02	0.017977879	0.101106045
$ au_{2,1}$	0.01	0.008884672	0.111532829
$\delta_{1,2}$	0.01	0.010612074	0.061207387
$\delta_{2,1}$	0.01	0.010150026	0.015002581
$\zeta_{1,2}$	0.01	0.002004724	0.799527586
$\zeta_{2,1}$	0.01	0.017996054	0.79960542

#### 3.2 Real Data

Next, we validate the performance of the method with real data that were collected using a list of data sets that the Ministry of Health and Social Protection of Colombia makes available to citizens, freely and without restrictions, so that they can reuse or create services derived from them. This information is organized by months and years and is found in the COVID-19 Colombia Case Bulletins available in Boletines Casos COVID-19 (2020). The complete query of the data sets is available on the Open Data Portal of the Colombian State available at the National Institute of Health, Colombia (Instituto Nacional de Salud, 2021).

To estimate the parameters of the proposed model, and to carry out the simulations and their analysis, we focus on the information available for the two main cities of Colombia, Bogotá and Medellín. The data set includes daily cases of infected, recovered, and deceased people, specifically, the information from January 2021 to December 2021 was selected. After carrying out an exhaustive cleaning of the data set, to simulate the number of susceptible people, we used

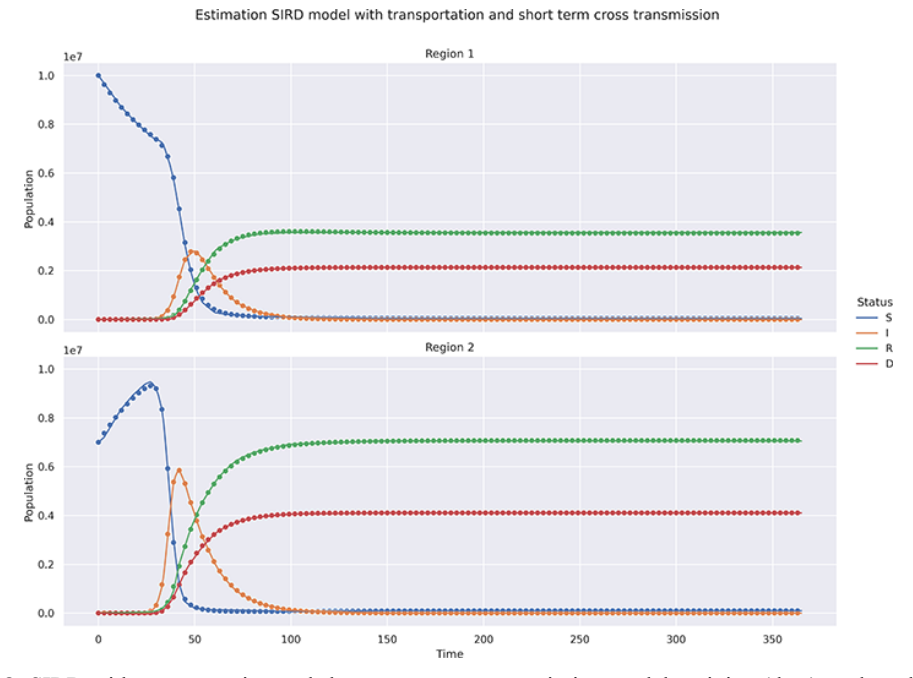


**FIG. 8:** SIRD with transportation and short-term cross transmission model, training (dots), and prediction (line) using synthetic data with 5% of noise

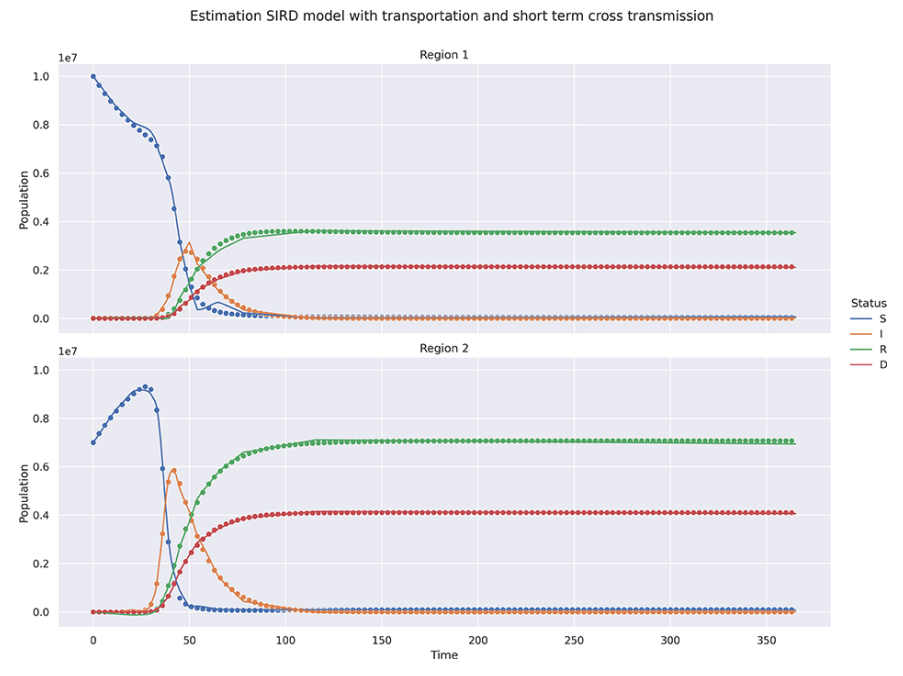
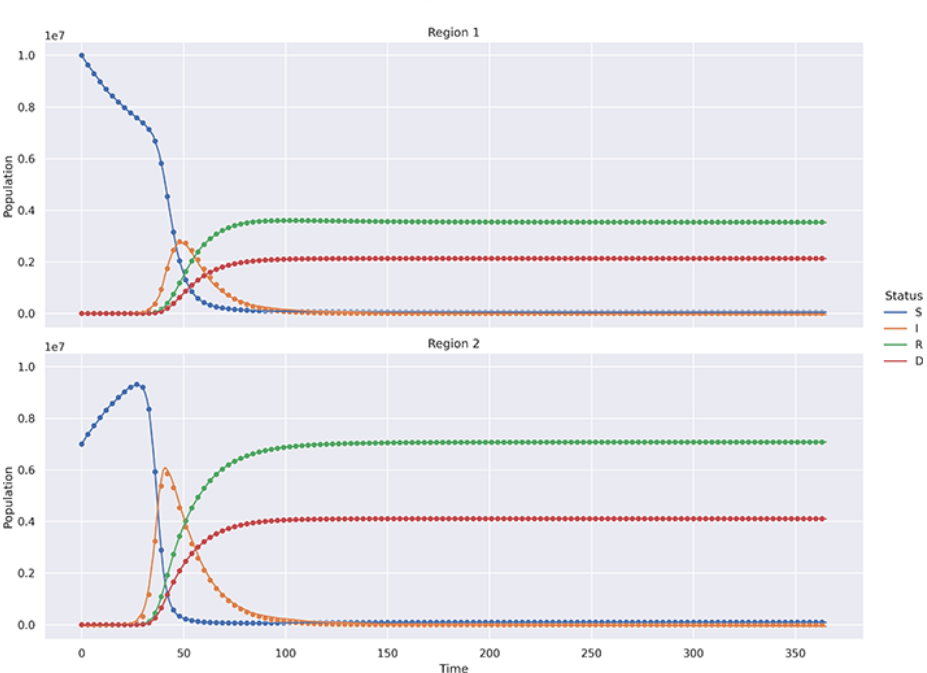


**FIG. 9:** SIRD with transportation and short-term cross transmission model, training (dots), and prediction (line) using synthetic data with 10% of noise



Estimation SIRD model with transportation and short term cross transmission

FIG. 10: SIRD with transportation and short-term cross transmission model, training (dots), and prediction

the demographic projection of the National Administration Department of Statistics of Colombia (DANE, 2018), where it is estimated that the approximate population of the city of Bogotá is 7,871,075, while the estimated number of inhabitants in the city of Medellín is 4.055.296. Due to the difficulty in obtaining real and precise information for the estimation of the value of the transport flow parameter  $\tau_{i,j}$  from Bogotá to Medellín and vice versa, we have assumed and taken the values from Pérez (2022). Likewise, in the case of the parameter  $\zeta_{i,j}$ , the values were assumed given the impossibility of obtaining said values in the literature and in the data available for the study cities. Results with both transportation models are illustrated in Figs. 11 and 12. These were obtained using similar hyperparameters that we used for synthetic data but since we are using a smaller data set (only ten training points) we decided to give more weight to the data loss function. While approximations are not perfect on the training data set, our models can still capture the underlying behavior.

As it is possible to observe by calculating the relative error, comparing the actual (and/or assumed) parameter values and the projected values, the estimates of the proposed model are not exact; this is possibly associated with the uncertainty of the assumed values for  $\tau_{i,j}$  and  $\zeta_{i,j}$ . However, our models can capture the underlying behavior of the population studied.

## 4. DISCUSSION AND CONCLUSIONS

(line) using synthetic data, but infected data are missing

In this work, we investigate the dynamics of infectious diseases through mathematical models that incorporate the impact of travel. The novelty of the work is to employ a computational approach through neural networks. Specifically, we introduced a DINNs approach that is fast

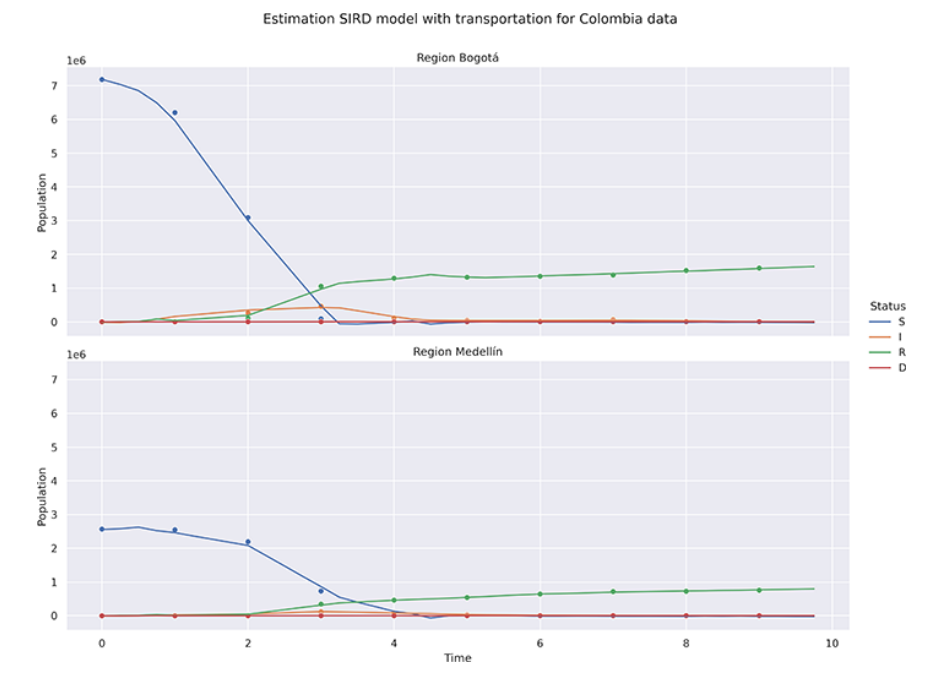
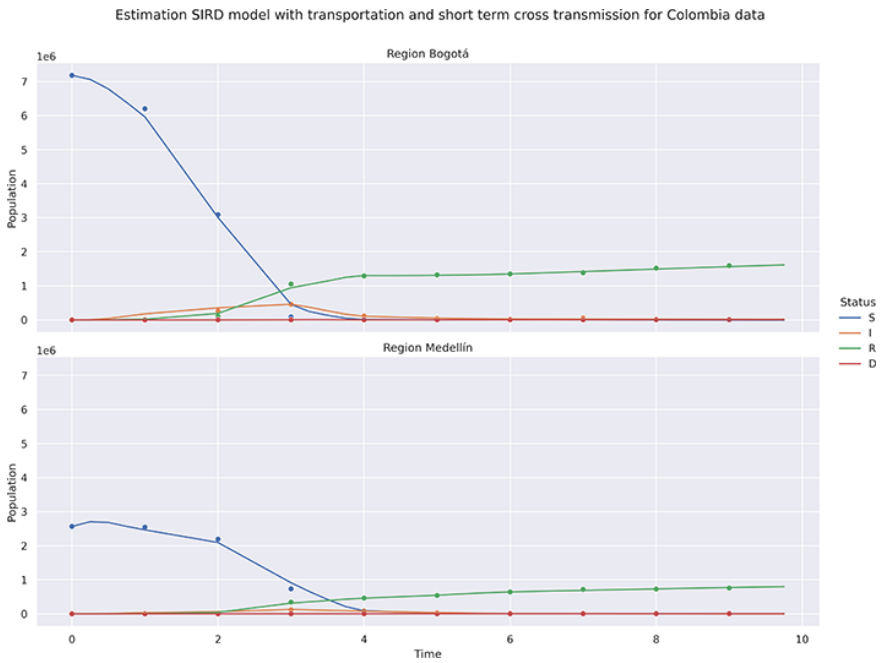


FIG. 11: SIRD with transportation model, training (dots), and prediction (line) using Colombia COVID-19 real data



(line) using Colombia COVID-19 real data

and robust, and is an extensible tool for parameter estimation. We derive the basic reproduction number for the basic SIRD with a transport model between two cities. We also validate the model in the presence of synthetic data. Our numerical results show that the method is reliable even in the presence of noise as well as missing data situations. While our method is shown to be robust, there is still a need to find better hyperparameters for the neural network to minimize synthetic data errors. Future works will include hyperparameter optimization methods. Our hypothesis for explaining why the flow parameters in the short-term cross transmission experiments did not perform well is related to the decomposition of loss functions. Artificial neural networks are still considered black boxes (or gray boxes) as we can predict how they learn from the data and the ODEs residuals. Considering that  $\zeta_{1,2}$  and  $\zeta_{2,1}$  are small values and their contribution to the system of equations (3) could be negligible, we hypothesize that the optimization algorithm prefers to move in directions where other parameters contribute in a larger sense to the loss function. Finally, this work indicates the need for more training data that can help improve the optimization process and better identify nonlinear behaviors. Additionally, as evidenced from the real data, due to the existing uncertainty around parameters that have been assumed, such as  $\tau_{i,j}$  and  $\zeta_{i,j}$ , it is essential to implement methodologies that can quantify said variability, as do the models that include random disturbances within the models that use stochastic differential equations. Parametric estimations of models that include stochastic approaches such as Ríos-Gutiérrez et al. (2021) or Niño-Torres et al. (2022) have been made. We hope to include adding stochasticity to our models and extending to long-term transmission in our forthcoming work.

#### **AVAILABILITY OF DATA AND MATERIAL**

Code and experiments are available at the following GitHub public URL. If specific additional details are needed, the authors welcome emails from the readers.

Webpage: https://github.com/aoguedao/dinn\_covid19

### **ACKNOWLEDGMENTS**

This research was partly supported by the last author's grants from the National Science Foundation, DMS-2031029 and DMS-2230117, and the financial support by Directorate-Bogotá campus (DIB), Universidad Nacional de Colombia under Project No. 51145 received by the second and third authors.

## **CONFLICT OF INTEREST**

The authors declare that they have no conflict of interest. Authors have no relevant financial or nonfinancial interests to disclose. The authors have no competing interests to declare that are relevant to the content of this article.

#### REFERENCES

Boletines Casos COVID-19, C., Boletines Casos COVID-19, Colombia, accessed from https://www.ins.gov.co/BoletinesCasosCOVID19Colombia/Forms/AllItems.aspx, 2020.

Brauer, F., Castillo-Chavez, C., and Castillo-Chavez, C., *Mathematical Models in Population Biology and Epidemiology*, Vol. 2, Berlin: Springer, 2012.

Calafiore, G.C., Novara, C., and Possieri, C., A Time-Varying SIRD Model for the COVID-19 Contagion in Italy, Annu. Rev. Control, vol. 50, pp. 361–372, 2020.

- Castillo-Chavez, C., Mathematical and Statistical Approaches to AIDS Epidemiology, Vol. 83, Berlin: Springer Science & Business Media, 2013.
- Chowell, G., Diaz-Duenas, P., Miller, J., Alcazar-Velazco, A., Hyman, J., Fenimore, P., and Castillo-Chavez, C., Estimation of the Reproduction Number of Dengue Fever from Spatial Epidemic Data, *Math. Biosci.*, vol. 208, no. 2, pp. 571–589, 2007.
- Coronavirus, W., WHO Coronavirus (COVID-19) Dashboard, accessed from https://covid19.who.int/, 2021.
- Cuomo, S., di Cola, V.S., Giampaolo, F., Rozza, G., Raissi, M., and Piccialli, F., Scientific Machine Learning through Physics-Informed Neural Networks: Where We Are and What's Next, *J. Sci. Comput.*, vol. **92**, Article ID 88, 2022.
- DANE, C., Censo Nacional De Poblacion Y Vivienda 2018, accessed from https://www.dane.gov.co/index.php/estadisticas-por-tema/demografia-y-poblacion/censo-nacionalde-poblacion-y-vivenda-2018, 2018.
- Diekmann, O., Heesterbeek, J.A.P., and Metz, J.A., On the Definition and the Computation of the Basic Reproduction Ratio R<sub>0</sub> in Models for Infectious Diseases in Heterogeneous Populations, *J. Math. Biol.*, vol. **28**, no. 4, pp. 365–382, 1990.
- Dye, C. and Gay, N., Modeling the SARS Epidemic, Science, vol. 300, no. 5627, pp. 1884–1885, 2003.
- Hernández, A., Olawoyin, O., Taipe, D., Cruz-Aponte, M., Morales Butler, E., and Mubayi, A., The Spatial-Temporal Dynamics of Chikungunya in Most Affected Ecuadorian Provinces, Tech. Rep., 2016. DOI: 10.13140/RG.2.2.28772.88969
- Instituto Nacional de Salud, C., Coronavirus (COVID-19) en Colombia, accessed from https://www.ins.gov.co/Noticias/Paginas/Coronaviruss.aspx, 2021.
- Kermack, W.O. and McKendrick, A.G., A Contribution to the Mathematical Theory of Epidemics, *Proc. R. Soc. London, Ser. A*, vol. **115**, no. 772, pp. 700–721, 1927.
- Niño-Torres, D., Ríos-Gutiérrez, A., Arunachalam, V., Ohajunwa, C., and Seshaiyer, P., Stochastic Modeling, Analysis, and Simulation of the COVID-19 Pandemic with Explicit Behavioral Changes in Bogotá: A Case Study, *Infect. Disease Model.*, vol. 7, no. 1, pp. 199–211, 2022.
- Padmanabhan, P., Seshaiyer, P., and Castillo-Chavez, C., Mathematical Modeling, Analysis and Simulation of the Spread of Zika with Influence of Sexual Transmission and Preventive Measures, *Lett. Biomath.*, vol. **4**, no. 1, pp. 148–166, 2017.
- Pérez, N.H., 2021 Reactivación Empresarial de Solways Colombia tras la Implementación de Protocolos de Bioseguridad por Covid en Cartagena Colombia, Trabajos de Grado, Universidad del Rosario, 2022.
- Raissi, M., Perdikaris, P., and Karniadakis, G.E., Physics-Informed Neural Networks: A Deep Learning Framework for Solving Forward and Inverse Problems Involving Nonlinear Partial Differential Equations, J. Comput. Phys., vol. 378, pp. 686–707, 2019a.
- Raissi, M., Ramezani, N., and Seshaiyer, P., On Parameter Estimation Approaches for Predicting Disease Transmission through Optimization, Deep Learning and Statistical Inference Methods, *Lett. Biomath.*, vol. 6, no. 2, pp. 1–26, 2019b.
- Ríos-Gutiérrez, A., Torres, S., and Arunachalam, V., Studies on the Basic Reproduction Number in Stochastic Epidemic Models with Random Perturbations, *Adv. Diff. Eq.*, vol. **2021**, no. 1, p. 288, 2021.
- Shaier, S., Raissi, M., and Seshaiyer, P., Data-Driven Approaches for Predicting Spread of Infectious Diseases through DINNs: Disease Informed Neural Networks, *Lett. Biomath.*, vol. **9**, no. 1, pp. 71–105, 2022.

- Van den Driessche, P. and Watmough, J., Further Notes on the Basic Reproduction Number, in *Mathematical Epidemiology*, Lecture Notes in Mathematics, F. Brauer, P. Driessche, and J. Wu, Eds., Berlin: Springer, pp. 159–178, 2008.
- Yazdani, A., Lu, L., Raissi, M., and Karniadakis, G.E., Systems Biology Informed Deep Learning for Inferring Parameters and Hidden Dynamics, *PLoS Comput. Biol.*, vol. **16**, no. 11, p. e1007575, 2020.